

H. VAHABI, R. SONNIER, B. OTAZAGHINE, G. LE SAOUT, J. M. LOPEZ-CUESTA<sup>\*)</sup>

Centre de Recherche C2MA (Centre des Matériaux des Mines d'Ales)  
Ecole des Mines d'Ales 6 avenue de Clavieres, F-30319 Ales cedex, France

## Nanocomposites of polypropylene/polyamide 6 blends based on three different nanoclays: thermal stability and flame retardancy

**Summary** — The influence of various layered silicates: sepiolite (needle-like structure), halloysite (nanotube structure) or organomodified montmorillonite (lamellar structure) in combination with phosphorous flame retardants [ammonium polyphosphate (APP) and aluminum diethylphosphinate (OP)] on the properties and morphologies of compatibilized PP/PA 6 blends has been investigated. Thermal degradation and fire retardancy of these blends were explored using TGA, cone calorimeter, pyrolysis flow combustion calorimeter (PCFC). Morphology of nanocomposites and residues as well of the chemical structure formed after cone calorimeter tests were investigated. The sepiolite/APP composition led to the better fire performance through the formation of a large amount of charred and expanded residue reinforced by the sepiolite fibres. The better compactness of this residue than that of the montmorillonite/APP one enables to account for the interest of sepiolite, whereas montmorillonite exerts the better fire retardant role, alone in the polymer blend.

**Keywords:** mineral filler, nanocomposite, halloysite, sepiolite, flame retardancy.

### NANOKOMPOZYTY NA BAZIE MIESZANINY POLIPROPYLENU/POLIAMIDU 6 Z UDZIAŁEM TRZECH RÓŻNYCH NANOGLINEK: STABILNOŚĆ TERMICZNA I OGNIODPORNOŚĆ

**Streszczenie** — Badano wpływ różnych warstwowych krzemianów: sepiolitu (struktura iglasta), haloizytu (struktura nanorurek) i organicznie modyfikowanego montmorylonitu (struktura płyt-kowa), użytych w układzie z fosforowymi uniepalniaczami [poli(fosforanem amonu) (APP) lub dietylofosfiną glinu (OP)] na właściwości termiczne i ogniodporność kompatybilizowanej mieszaniny polimerów PP/PA 6. Degradację termiczną oraz odporność na ogień oceniano metodą TGA, za pomocą kalorymetru stożkowego a także mikrokalorymetru pirolizy i spalania (PCFC). Morfologię nanokompozytów oraz strukturę powstałej pozostałości po testach kalorymetrycznych badano za pomocą skaningowej mikroskopii elektronowej (SEM). Zastosowanie układu sepiolit/APP prowadzi do utworzenia na powierzchni próbki największej ilości barierowej, zwęglonej pozostałości, dodatkowo wzmacnionej włóknami sepiolitowymi, co umożliwia najlepszą ochronę przed ogniem otrzymanego nanokompozytu. Większa spoistość tej pozostałości niż uzy-skanej w przypadku stosowania układu montmorylonit/APP skłania do większego zainteresowania glinką sepiolitową, mimo iż sam montmorylonit, użyty jako napełniacz PP/PA 6 jest skuteczniejzym środkiem uniepalniającym.

**Słowa kluczowe:** napełniacz mineralny, nanokompozyt, haloizyt, sepiolit, opóźniacz palenia.

### INTRODUCTION

Since the last decade, the use of nanoparticles in polymers in order to improve their fire reaction has become an attractive field of research. Different parameters, such as chemical composition, microstructure, specific surface area, shape, particle size distribution, surface modification as well as their dispersion state in the matrix govern their contribution to flame retardancy [1, 2]. Among

nano particles incorporated in polymers, organomodified layered silicates (OMLS) are of prime interest due to their availability, cost and contribution to flame retardancy [3]. Combinations of organomodified montmorillonites (OMMT) with various flame retardants, and particularly phosphorous compounds have attracted special attention [4] regarding the improvement of fire performance achieved for various polymers. Different mechanisms have been suggested to explain the effect of OMMT on flame retardancy as well as the interactions with phosphorous compounds acting as components of intumescent flame retardant (IFR) compositions [5, 6]. Hence, it

<sup>\*)</sup> Corresponding author; e-mail: Jose-Marie.Lopez-Cuesta@mines-ales.fr

appears likely that these interesting results will prompt researchers to investigate new combinations of layered silicates with phosphorous compounds. This paper focuses particularly on the comparison between three kinds of layered silicates presenting different morphologies, as well as their combinations with phosphorous compounds to improve the fire reaction of polypropylene/polyamide 6 blends in which polypropylene is the main component. PP/PA 6 blends have been used in the industry (*e.g.* ORGALLOYS from ARKEMA) since many years. Various solutions aiming to improve the fire retardancy of these blends which contains also compatibilizing agents can be considered. The interest of IFR systems has yet been proved for polyolefins and IFR systems containing PA 6 as char promoter have been proposed [7]. Moreover, it has been shown that IFR systems containing ammonium polyphosphate (APP) and PA 6 could generate synergistic effects on flame retardancy when combined with organomodified montmorillonites [8–10]. Nevertheless, even if the interest of modified sepiolite in combination with other kind of IFR (pentaerythritol instead of PA 6) in PP has been highlighted by Huang *et al.* [11], no investigation has been made about a comparison between various layered silicates having different microstructures, combined with IFR systems in PP. It had been shown in some cases that lamellar microstructures could be superior to fibrous, acicular, or tubular morphologies [6], due to their potential ability to build a tile-like structure at the surface of polymer when exposed to a heat source leading to its combustion. Nevertheless, other phenomena have to be taken into account such as:

- catalytic effects of silicate surface, particularly when surface modified,
- influence on the morphology of the charred structure formed at the surface of material residue,
- possible reactions occurring at high temperatures between the layered silicates and the phosphorous FR as it has been shown with nanooxides [12].

In this work, comparisons have been made with the three types of layered silicates alone in a PP/PA 6 compatibilized blend and also in combinations with the two phosphorous FR. The organomodified montmorillonite has been selected to enable a good dispersion in the PP phase through the use of SEBS-g-MA (SGM) which plays also the role of compatibilizing agent in the PP/PA 6 blend. Non-modified sepiolite and halloysite have been used. This last kind of layered silicate has also been selected since some authors have shown that it could exert a flame retardant action in various polymers [13].

## EXPERIMENTAL

### Materials

Polypropylene (PP) (SABIC®-576P) and polyamide 6 (PA 6) (Rhodia C216-Technyl®) were used as polymer blend components with the following constant ratio

PP/PA 6 80:20. SEBS-g-MA (Kraton FG 1901-named as SGM) was used as blend compatibilizer. Halloysite (named as HNT) was provided by Imerys Tableware New Zealand Ltd. Pangel®-S9 Sepiolite (named as Sep.) from Tolsa (Spain) was supplied by Lavollée S.A. (France). An organomodified montmorillonite, modified with a quaternary ammonium (dimethyldihydrogenated tallow alkyl quaternary ammonium salt, named as N5) was provided by Southern Clay Products (Nanofil®5). The following phosphorous flame retardants supplied by Clariant were used as powders: an ammonium polyphosphate (AP 412 named as APP) and an organic aluminium phosphinate based composition containing a nitrogen compound acting as synergistic agent (Exolit OP1311).

### Samples preparation

All blends were prepared in one step using a co-rotating twin screw extruder (Clextral BC 21, screw speed = 250 rpm, melt zone temperature = 180–240 °C). All nanoparticles were introduced in the molten polymer blend.

**Table 1.** Sample names and compositions<sup>a)</sup>

Sample code	Composition, wt. %				
	PP80 %/ PA20 %	SGM	Sep	HNT	N5
PP/PA	100	—	—	—	—
PP/PA/SGM	95	5	—	—	—
PP/PA/SGM/Sep	90	5	5	—	—
PP/PA/SGM/HNT	90	5	—	5	—
PP/PA/SGM/N5	90	5	—	—	5

<sup>a)</sup> SGM = SEBS-g-MA, Sep — sepiolite, HNT — halloysite, N5 — Nanofil®5.

The pellets were injection molded using a Krauss Maffei 50T apparatus ( $T = 200\text{--}240\text{ }^{\circ}\text{C}$ , mold temperature = 80 °C) in order to obtain square sheet specimens  $100 \times 100 \times 4\text{ (mm}^3\text{)}$ . The sample names and compositions are given in Table 1 and Table 2. Prior to the processing, PA 6 and SEBS-g-MA were dried at 80 °C in a vacuum oven for 12 hours. Sepiolite, Nanofil®5 and Halloysite were also dried at 350 °C, 110 °C and 250 °C, respectively, to remove water physically bound.

### Methods of testing

— Thermogravimetric analysis (TGA) data were collected with a PerkinElmer Pyris-1 TGA instrument, under nitrogen, at 10 °C/min, from 50 °C to 900 °C.

— Evaluation of the flammability properties was made using Pyrolysis Combustion Flow Calorimeter (PCFC) and Cone Calorimeter devices manufactured by Fire Test Technology (FTT). For PCFC tests, the samples (1–4 mg) are heated at 1 °C/s from 20 °C to 750 °C in a pyrolyzer and the degradation products are transported by an inert flux, and then mixed with oxygen before

**T a b l e 2.** Sample names and compositions<sup>a)</sup>

Sample code	Composition, wt. %						
	PP80 %/PA20 %	SGM	Sep	HNT	N5	APP	OP
PP/PA/SGM/APP	80	5	—	—	—	15	—
PP/PA/SGM/OP	80	5	—	—	—	—	15
PP/PA/SGM/APP/Sep	75	5	5	—	—	15	—
PP/PA/SGM/OP/Sep	75	5	5	—	—	—	15
PP/PA/SGM/APP/HNT	75	5	—	5	—	15	—
PP/PA/SGM/OP/HNT	75	5	—	5	—	—	15
PP/PA/SGM/APP/N5	75	5	—	—	5	15	—
PP/PA/SGM/OP/N5	75	5	—	—	5	—	15

<sup>a)</sup> APP — ammonium polyphosphate, OP — organic aluminium phosphinate.

entering a combustor at 900 °C where the decomposition products are completely burnt. Heat release rate (*HRR*) is measured as function of temperature according to oxygen depletion method (13.1 MJ of energy is released when 1 kg of oxygen is used according to Huggett's relation). Cone calorimeter tests were carried out on the square sheet specimens using an incident heat flux of 35 kW/m<sup>2</sup>, according to ISO 5660-1 standard.

— All images were obtained using a scanning electron microscopy (FEI Quanta 200 SEM) under high vacuum at a voltage of 15.0 kV with a spot size of 3 mm and a working distance of 8.2 mm (all samples were cryo-fractured).

— X-ray diffraction (XRD) data were collected using a BRUKER Advance D8 diffractometer in a 0-0 configuration employing the CuK $\alpha$  radiation ( $\lambda = 1.54 \text{ \AA}$ ) with a fixed divergence slit size 0.6° and a rotating sample stage. The samples were scanned between 2.5° and 50° with the VANTEC-1 detector. The qualitative analysis was performed with the XPert High Score Plus software (version 2.1).

## RESULTS AND DISCUSSION

### Microstructures and properties of silicate layer nanocomposites

The first part of this work was devoted to the influence of three different geometries of layered silicates [sepiolite

(needle-like microstructure), halloysite (nanotube microstructure) or organomodified montmorillonite (lamellar microstructure)] on flammability of PP/PA/SEBS-g-MA blend. The formulation was carried out without the phosphorus FR in order to evaluate the influence of different geometries of these clays. The microstructures of the layered silicates in the PP/PA/SGM blend are shown in Fig. 1.

It can be observed that all the silicates are dispersed in the blend even if some aggregates can be noticed. Consequently, it can be considered that nanostructures have been achieved. The presence of the organomodifier in Nanofil®5 seems not to modify the size of PA 6 nodules in the PP matrix. In order to investigate the exfoliation of montmorillonite in the matrix, XRD experiments have been performed (Fig. 2). In the N5 sample, the intercalation agent (dimethyl-distearyl-ammonium chloride) expands the interlayer spacing d001 of the montmorillonite up to 2.5 nm. We can notice a swelling of the phase (d001 = 2.8 nm) when the sample is heated up to 220 °C (temperature of the process). On preparing the PP/PA 6 blends sample, an increase of the basal spacing to 3.1 nm is observed. No complete montmorillonite exfoliation has taken place as previously reported in polymer blends based on polyethylene and N5 [14].

TGA curves are presented in Fig. 3. While HNT and Sep compositions decomposes similarly to the polymer blend up to 480 °C, and show the presence of a residue af-

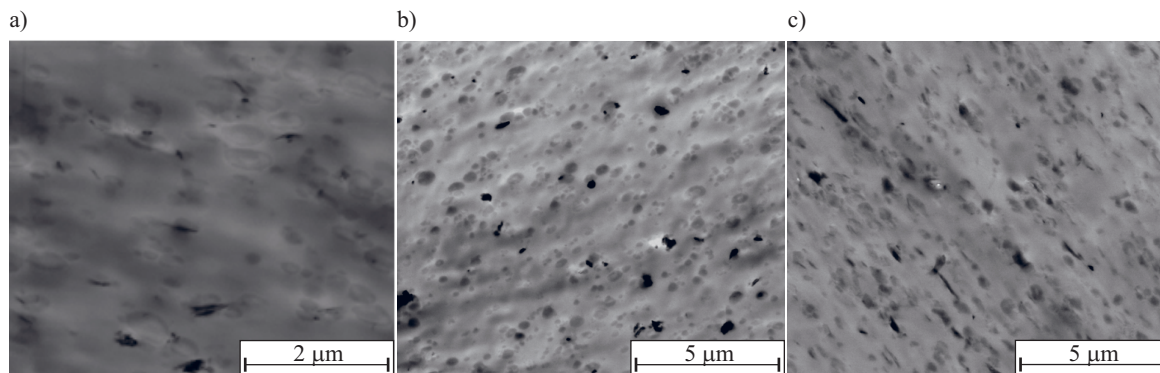


Fig. 1. SEM micrographs of nanocomposites: a) PP/PA/SGM/Sep, b) PP/PA/SGM/HNT, c) PP/PA/SGM/N5

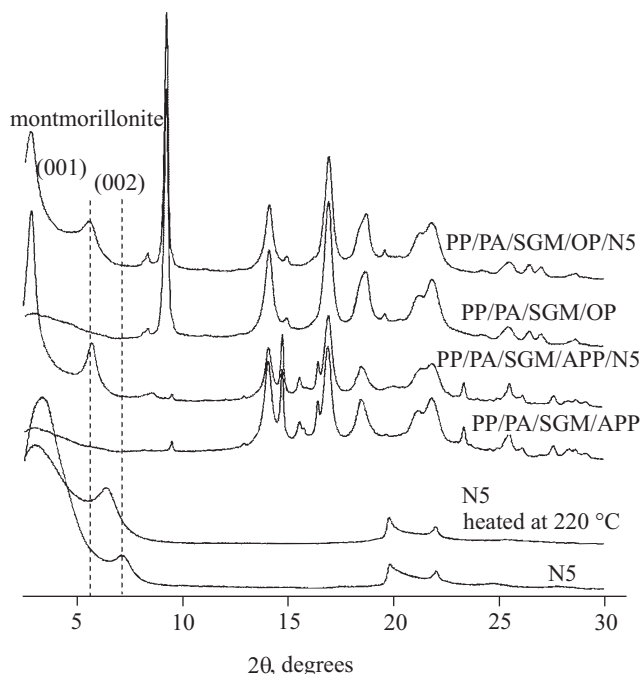


Fig. 2. XRD patterns of organomodified montmorillonite (N5) and PP/PA 6 blends with and without N5

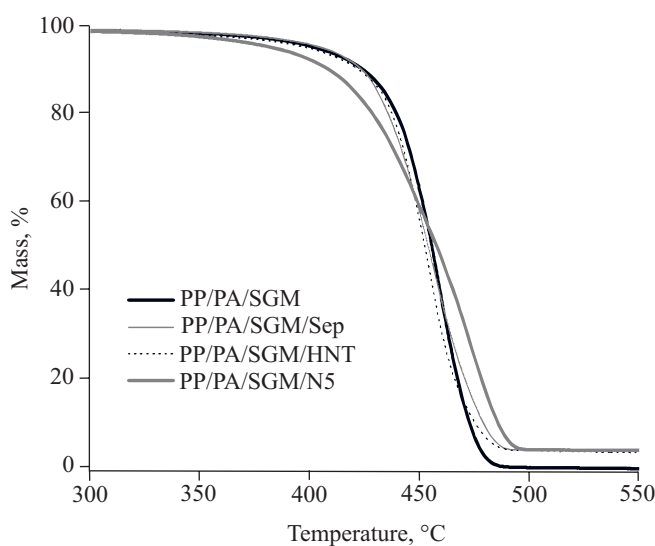


Fig. 3. TGA curves of PP/PA/SGM polymer blend and its nanocomposites

ter this temperature, Nanofil®5 composition decomposes at lower temperature (close to 350 °C) but appears more stable than all other compositions from 450 °C. Moreover, a final residue close to 5 wt. % is obtained for all compositions. It can be noticed that residue of Nanofil®5 composition contains a little char fraction since this organomodified layered silicate contains 30 wt. % of organic fraction.

The heat release (HRR) curves of the nanocomposites at cone calorimeter are presented in Fig. 4. These results clearly showed that Nanofil®5 (platelet geometry) significantly decreases the peak of HRR (around 50 %) compared to Sep or HNT, which seems to have no effect on pHRR reduction at this percentage of incorporation.

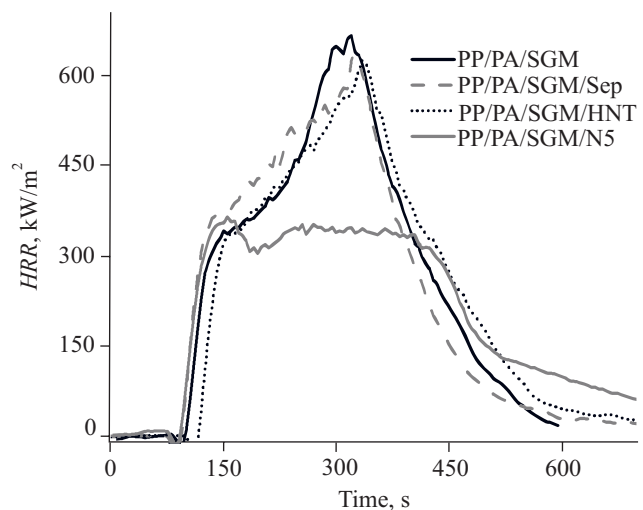


Fig. 4. HRR curves obtained from cone calorimeter test

Moreover, the total heat released (THR) at 500 °C appears slightly lower for Nanofil®5 composition, in comparison with this of the unfilled polymer blend (Table 3). However, it is well known that generally the incorporation of nanoparticles allows HRR values to be reduced but not the THR [15–17]. Time to ignition (TTI) is not modified by the incorporation of Nanofil®5 and sepiolite, but it is increased of 20 % with halloysite. It can be suggested that the tubular structure of halloysite may increase the thermal diffusivity through the sample and thereby delay ignition. It is also recognized that there is no general rule about this parameter for the incorporation of nanoparticles in polymers.

Table 3. Cone calorimeter data for PP/PA/SGM polymer blends and its nanocomposites

Composition	TTI, s	pHRR, kW/m²	THR, MJ/m²
PP/PA/SGM	87	670	158
PP/PA/SGM/Sep	83	630	160
PP/PA/SGM/HNT	108	628	164
PP/PA/SGM/N5	83	365	154

These results concerning HRR values is in accordance with previous research works that showed the excellent performance of organomodified clays regarding reduction of pHRR, because of its effectiveness to build a protective mineral barrier at the surface of remaining material, hindering by a physical effect, the diffusion of volatile combustible from the filled blend and oxygen through it [15, 16]. The formation of a mineral barrier in case of organomodified montmorillonite after polymer ablation but also from the migration of the dispersed clay platelets towards the surface exposed to heat source [18]. Such kind of mechanism requires exfoliated or intercalated microstructures and was only highlighted for this type of nanoparticles

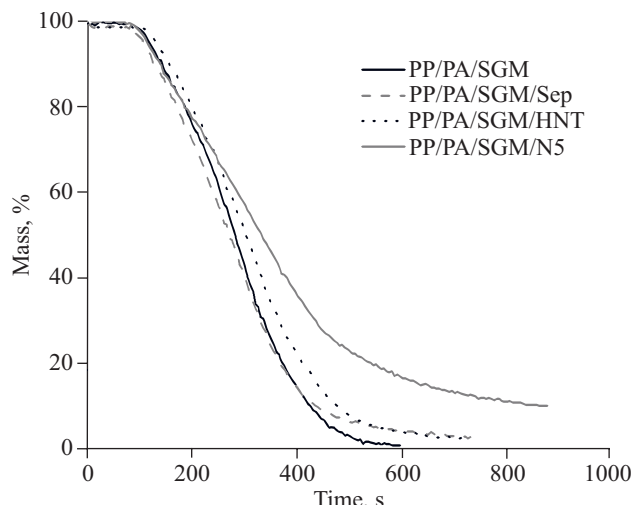


Fig. 5. Mass loss of samples at cone calorimeter test

centage of incorporation is quite always much higher than 20 wt. %.

In the case of the combined presence of layered silicates and phosphorous compounds, the formation of new compounds could modify the structure of the protective layer formed in presence of organomodified montmorillonite. Moreover, it can be expected that a protective layer could also be formed from the reaction of other kind of silicates with phosphorous compounds.

#### Microstructures and properties of multicomponent compositions

The SEM microstructures of the PP/PA/SGM/APP, PP/PA/SGM/OP and the six multicomponent composi-

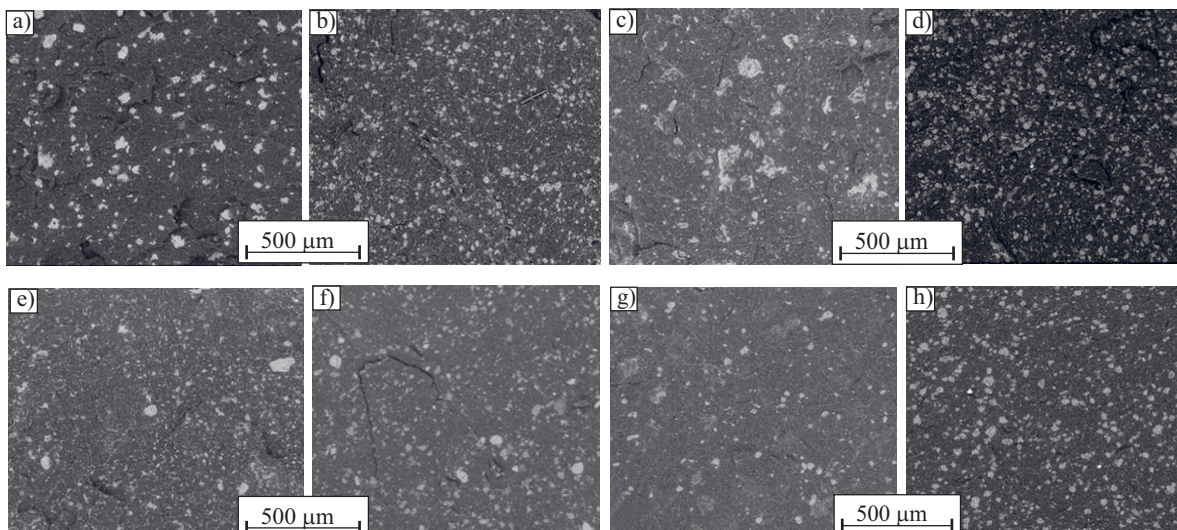


Fig. 6. SEM images of a) PP/PA/SGM/APP, b) PP/PA/SGM/OP, c) PP/PA/SGM/APP/Sep, d) PP/PA/SGM/OP/Sep, e) PP/PA/SGM/APP/HNT, f) PP/PA/SGM/OP/HNT, g) PP/PA/SGM/APP/N5, h) PP/PA/SGM/OP/N5

and not for other kind of silicates having different aspect ratio and different surface chemistry. Moreover, after thermal degradation of the organomodifier, montmorillonite exhibits an acidic surface, leading to enhanced catalytic activity, which promotes the formation of a charred structure reinforced by the clay platelets. The formation of this kind of barrier is confirmed here by the evolution of sample weight during the test (Fig. 5). The weight loss is slower for the composition with Nanofil®5 and the final residue at 800 s is significantly higher than the theoretical weight loss, taking into account the organic fraction (around 30 wt. %) of the organomodified montmorillonite. Conversely, for the other layered silicates, the weight of residue is close to this of the nanoparticle fraction in the polymer blend. Hence, sepiolite and halloysite seem not to exhibit any catalytic activity on the polymer blend degradation. It has to remind that in the various papers handling with the use of sepiolite and halloysite to exert a flame retardant action, their per-

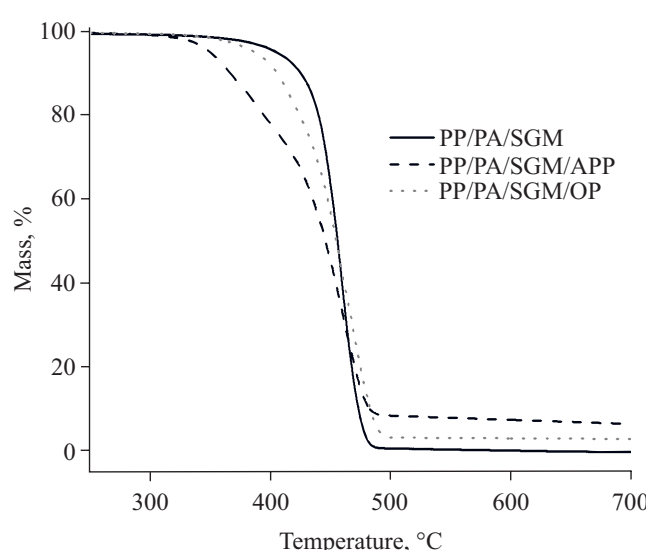


Fig. 7. TGA curves in nitrogen (10 °C/min) of PP/PA/SGM, PP/PA/SGM/APP and PP/PA/SGM/OP compositions

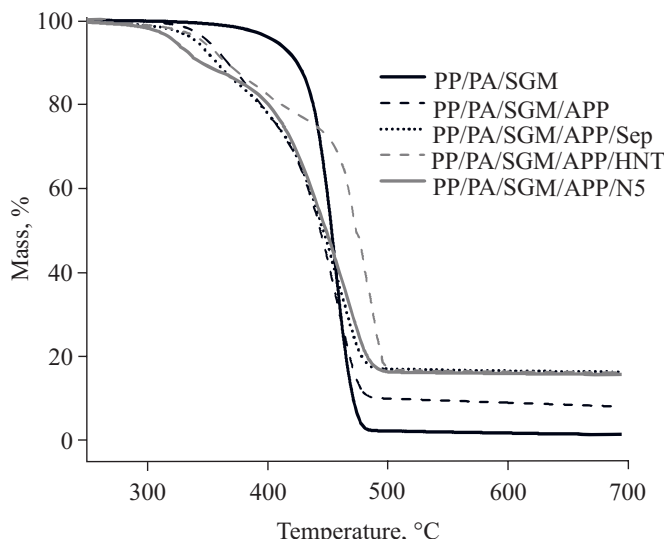


Fig. 8. TGA curves in nitrogen ( $10\text{ }^{\circ}\text{C}/\text{min}$ ) of PP/PA/SGM, PP/PA/SGM/APP, PP/PA/SGM/APP/Sep, PP/PA/SGM/APP/HNT, and PP/PA/SGM/APP/N5 compositions

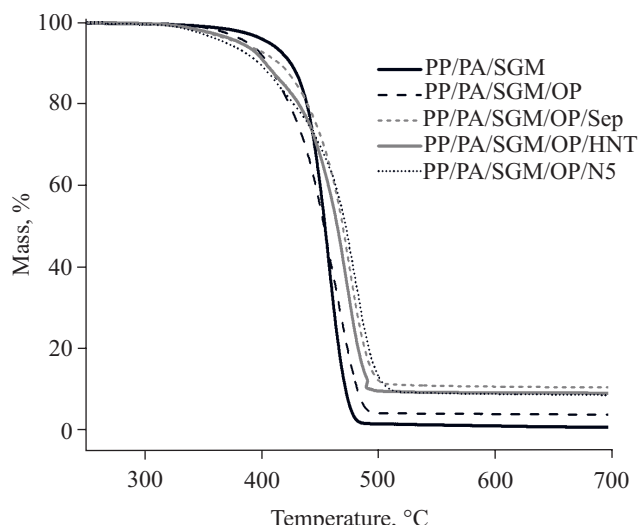


Fig. 9. TGA curves in nitrogen ( $10\text{ }^{\circ}\text{C}/\text{min}$ ) of PP/PA/SGM/OP/HNT and PP/PA/SGM/OP/N5 compositions

tions containing nanoparticles and phosphorous compounds are presented in Fig. 6. It can be observed that both APP and OP micronic particles are well dispersed in the polymer blend matrix. In the case of multicomponent compositions, only the PP/PA/SGM/APP/Sep compositions seem to present large aggregates higher than  $50\text{ }\mu\text{m}$ .

Thermogravimetric analysis (TGA) and derived TGA curves of the above compositions are shown in Figs. 7 to 9 and various TGA parameters are summarized in Table 4.

At first, it can be noticed that phosphorous flame retardants (FR) impair the thermal stability of polymer blend (Fig. 7). The effect is more important with APP since it is less thermally stable than OP [12, 19]. It can be also ascribed to possible reactions with PA 6, since PA 6 can play a role as charring agent in intumescent systems based on APP [5].

Table 4. TGA parameters of all samples under nitrogen

Sample code	$T_{onset}$ °C	$T_{10\%}$ °C	$T_{50\%}$ °C	Char residue at $700\text{ }^{\circ}\text{C}$ , wt. %
PP/PA	375	419	462	1.5
PP/PA/SGM	375	426	456	0.0
PP/PA/SGM/APP	320	366	445	6.3
PP/PA/SGM/OP	340	405	453	2.8
PP/PA/SGM/APP/Sep	310	357	447	14.8
PP/PA/SGM/OP/Sep	325	414	470	9.5
PP/PA/SGM/APP/HNT	320	363	476	14.6
PP/PA/SGM/OP/HNT	327	402	466	8.0
PP/PA/SGM/APP/N5	290	342	450	14.1
PP/PA/SGM/OP/N5	330	397	474	7.6

Two decomposition stages can be noticed in the TGA curve for the samples containing the layered silicates, particularly in the case of APP. The first stage ranges from  $300\text{ }^{\circ}\text{C}$  to  $400\text{ }^{\circ}\text{C}$  and can be ascribed to the phosphorous compound decomposition while the second one ranges from around  $400\text{ }^{\circ}\text{C}$  to  $520\text{ }^{\circ}\text{C}$  and seems to correspond to the decomposition of PP and PA 6.

In all cases, the onset temperature ( $T_{onset}$ ) is lower than this of the compatibilized blend. APP/N5 composition presents the lower onset temperature of the multicomponent compositions due to the degradation of the dimethyl dihydrogenated tallow alkyl quaternary ammonium salt.

APP/HNT composition presents the highest thermal stability from  $450\text{ }^{\circ}\text{C}$  (see  $T_{50\%}$  in Table 4), but except for this composition, all the blends containing OP exhibit a better thermal stability than these containing APP.

For all compositions containing a phosphorous FR, significant amounts of residue are formed after polymer degradation, particularly for sample containing APP. Moreover, taken into account the respective percentage of nanoparticles and phosphorous FRs, a synergistic effect on residue formation can be highlighted for all compositions, except this containing OP and halloysite, taking into account the organic fraction of N5.

Pyrolysis combustion flow calorimetry has proved to be an advantageous technique to investigate fire behavior on very small specimens. Moreover, it has been highlighted in the literature that PCFC is more adapted to study chemical decomposition processes than physical ones (mass or heat transfer barrier effects) taking place in the condensed phase [10–22].

The heat release rate (HRR) curves obtained from PCFC test are shown in Figs. 10 to 12 and the main parameters summarized in Table 5.

It appears that the presence of the SEBS-g-MA as compatibilizer in the PP/PA 6 blend tends to increase strongly the SumHRC (Heat Release Capacity). The incorporation of phosphorous compounds leads to a significant decrease of this value, particularly for OP. All APP compositions exhibit two peaks and the first one can be attributed to a first degradation stage of the polymer blend caused by reactions of APP with PA 6.

**T a b l e 5.** Main PCFC parameters

Sample code	SumHRC, J/g · K	THR, kJ/g
PP/PA	806	38
PP/PA/SGM	961	38
PP/PA/SGM/APP	831	36
PP/PA/SGM/OP	733	38
PP/PA/SGM/APP/Sep	695	30
PP/PA/SGM/OP/Sep	605	32
PP/PA/SGM/APP/HNT	788	33
PP/PA/SGM/OP/HNT	712	38
PP/PA/SGM/APP/N5	879	35
PP/PA/SGM/OP/N5	643	36

For each kind of phosphorous compound, its combined incorporation with layered silicates leads to a

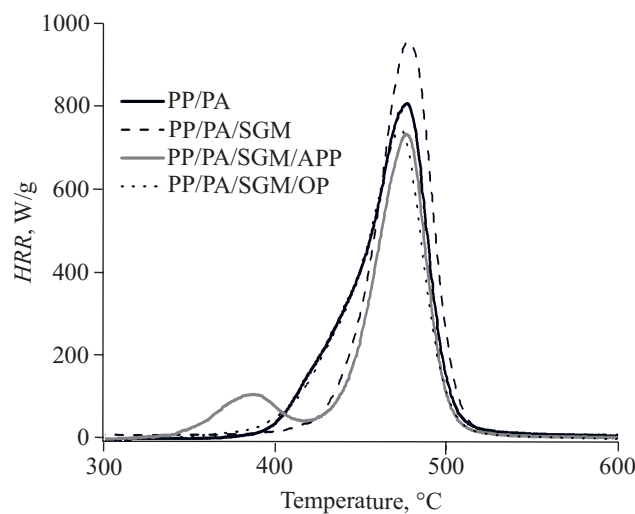


Fig. 10. Heat release rate curves of phosphorous FR compositions at PCFC test

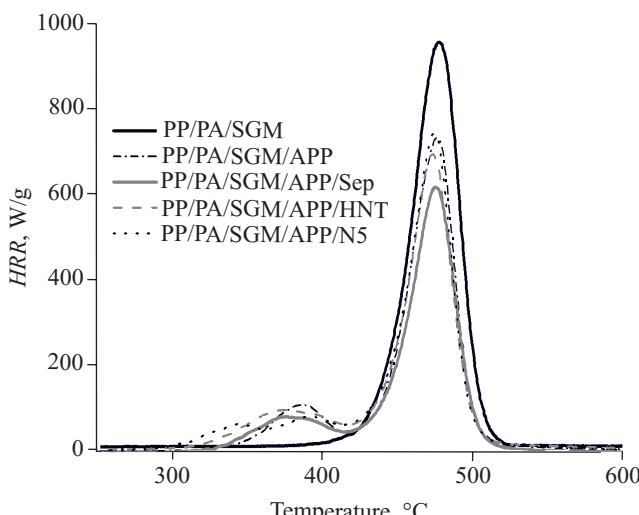


Fig. 11. Heat release rate curves of APP-based compositions at PCFC test

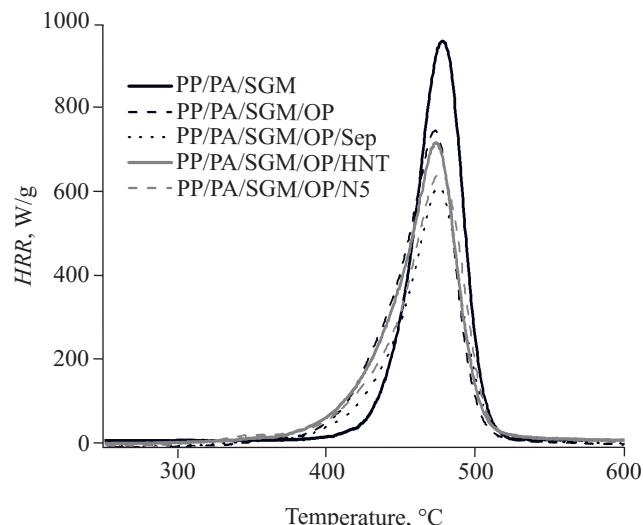


Fig. 12. Heat release rate curves of OP-based compositions at PCFC test

strong reduction in SumHRC, apart from the APP/N5 composition which seems to cause a decomposition of the polymer blend through a catalytic effect, in a lower temperature range in comparison with all other compositions. In fact, it could be noticed that APP/N5 composition shows the lowest  $T_{10\%}$  for all the compositions containing APP.

The highest reduction in SumHRC for multicomponent compositions in comparison with ones containing only phosphorous compounds is achieved with sepiolite (respectively 16 and 17 % for APP and OP).

**T a b l e 6.** Parameters of cone calorimeter test for all samples containing phosphorous compounds

Composition	TTI, s	pHRR-1 kW/m <sup>2</sup>	pHRR-2 kW/m <sup>2</sup>	THR MJ/m <sup>2</sup>
PP/PA/SGM	78	658	—	157
PP/PA/SGM/APP	72	238	350	148
PP/PA/SGM/OP	93	455	—	143
PP/PA/SGM/APP/Sep	60	148	140	131
PP/PA/SGM/OP/Sep	90	275	—	154
PP/PA/SGM/APP/HNT	61	406	332	144
PP/PA/SGM/OP/HNT	108	387	360	147
PP/PA/SGM/APP/N5	39	304	131	139
PP/PA/SGM/OP/N5	80	270	261	143

Cone calorimeter curves (Fig. 13, Fig. 14) and data (Table 6) confirm the interest of the combinations between the phosphorous compounds and sepiolite. The lowest pHRR value is obtained for the APP/Sep composition. In addition, OP/Sep exhibits a pHRR value very close to this of OP/N5 which presents the lowest value for the OP compositions. On the whole, the compositions with APP leads to a better fire reaction than OP ones. Times to ignition (TTI) appear slightly lower for APP compositions,

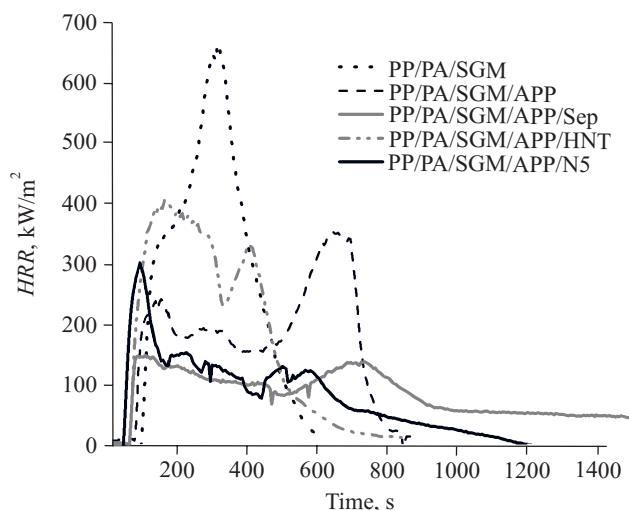


Fig. 13. Heat release rate curves of APP compositions at cone calorimeter test

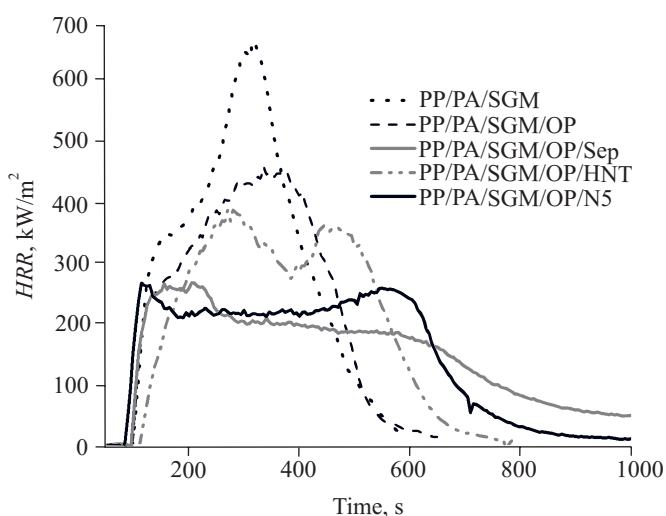


Fig. 14. Heat release rate curves of OP compositions at cone calorimeter test

the lowest values for both phosphorous compounds being obtained for N5 compositions.

THR values decrease for all compositions in comparison with this of the compatibilized blend. Lower THR values are observed for APP/Sep and APP/N5. In addition, it can be noticed that for OP compositions, the combination with nanoparticles does not enable to reduce the THR.

Finally, from the cone calorimeter experiments, it appears that sepiolite shows the better results, then modified montmorillonite, and finally halloysite, which present only a limited interest. So, despite its ability to promote char formation at moderate ramp temperature as for TGA, APP/HNT combination lead only to a limited mass of residue in comparison with APP/N5 and above all APP/Sep, in case of a strong temperature rise such as in cone calorimeter experiments. Fig. 15 shows the significant differences in mass loss between the three APP-based compositions containing the layered silicates.

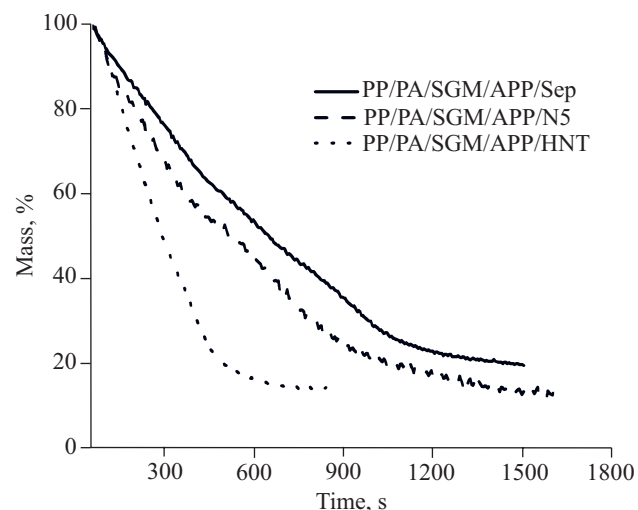


Fig. 15. Weight loss curves at cone calorimeter test for PP/PA/SGM/APP/Sep, PP/PA/SGM/APP/HNT and PP/PA/SGM/APP/N5 compositions

A comparison between PCFC and calorimeter data enables to account for the creation of a barrier effect through the formation of a protective layer. It was assumed that the barrier effect is only active in cone calorimeter test and negligible in PCFC due to the small sample size. Thus, it is supposed that the decrease of pHRR in cone calorimeter test (because of the incorporation of FR) should be higher (or at least equal to) than the decrease of pHRR {or Heat Release Capacity (HRC), [HRC is equal to the peak heat release rate (pHRR) divided by the heating rate] in PCFC [23].

Here, the ratio between the HRC value of the flame retarded polymer sample in PCFC test [P-FR (PCFC)] and the HRC value of the non retarded polymer [P (PCFC)] is named R1. (In this study, HRC is equal to pHRR due to presence of only one major peak of HRR and a heating rate of 1 °C/s).

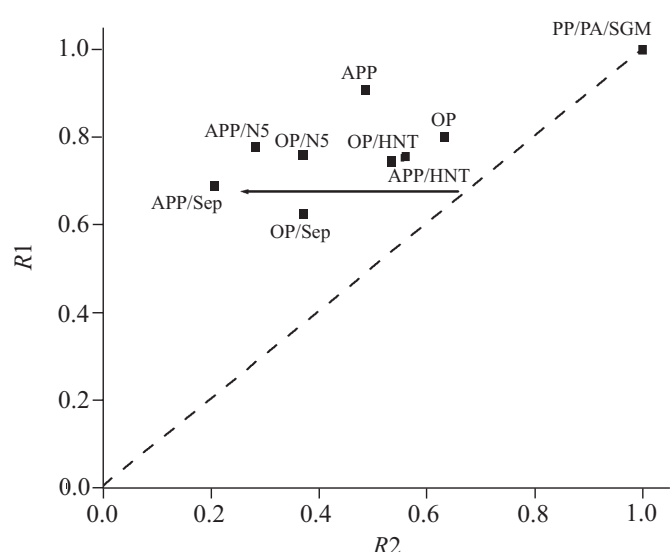


Fig. 16. R1 versus R2 representation

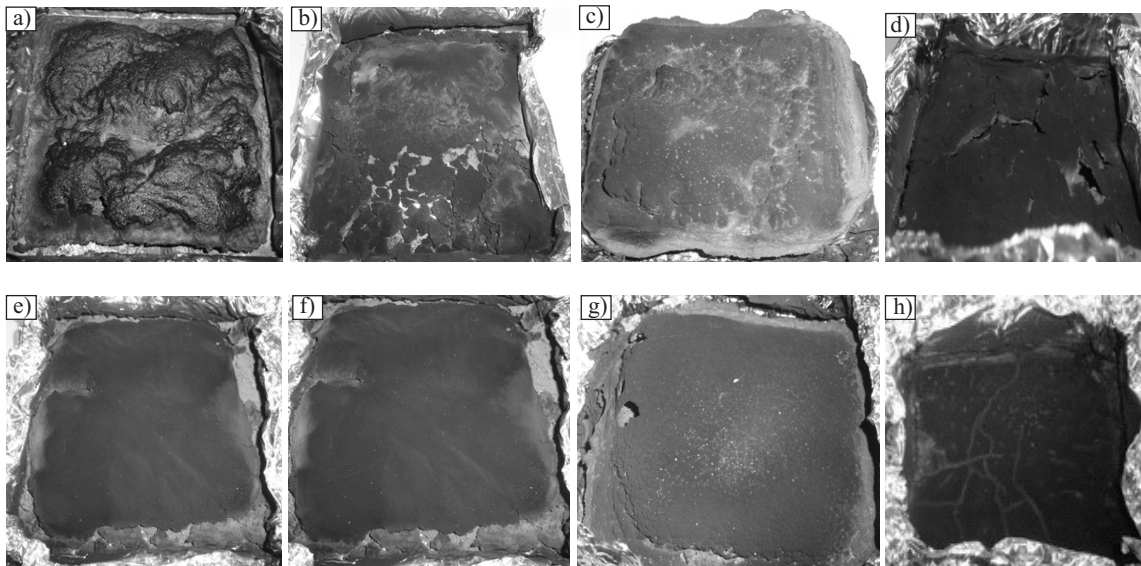


Fig. 17. Digital photographs of residues after cone calorimeter test: a) PP/PA/SGM/APP, b) PP/PA/SGM/OP, c) PP/PA/SGM/APP/Sep, d) PP/PA/SGM/OP/Sep, e) PP/PA/SGM/APP/HNT, f) PP/PA/SGM/OP/HNT, g) PP/PA/SGM/APP/N5, h) PP/PA/SGM/OP/N5

The ratio between the pHRR of the flame retarded polymer sample in cone calorimeter test [P-FR (cone calorimeter)] and the pHRR of the non retarded polymer [P (cone calorimeter)] is named  $R_2$ .

Figure 16 shows the representation of calculated  $R_2$  values (X-axis) versus calculated  $R_1$  values (Y-axis). For

all FR samples, the points are plotted above the dotted line  $R_1 = R_2$  (this line corresponds to a similar decrease in pHRR at cone calorimeter and at PCFC).

The extent of the discrepancies between experimental values and the dotted line  $R_1 = R_2$  indicates that the barrier effect plays an important role in flame retardancy of

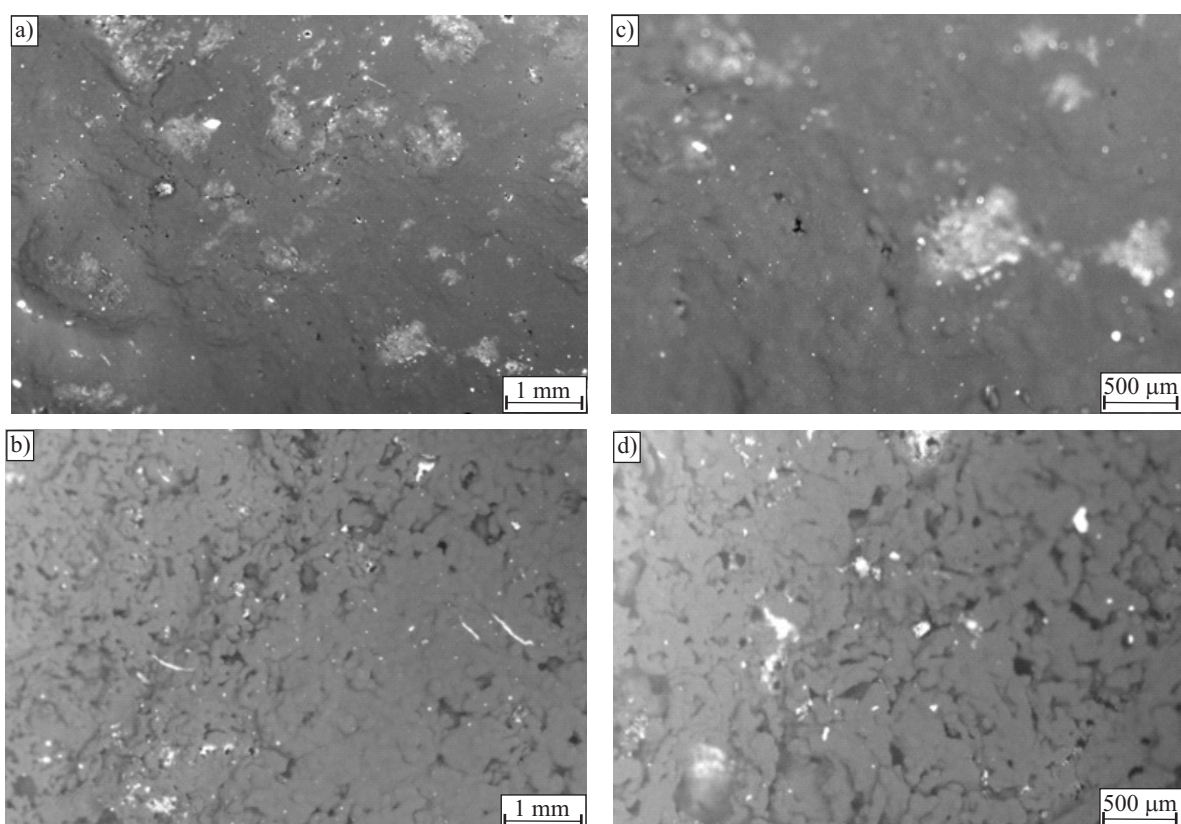


Fig. 18. Photographs of residue surfaces for PP/PA/SGM/APP/Sep (a, c) and PP/PA/SGM/APP/N5 (b, d)

these samples. The effect is particularly emphasized in the PP/PA/SGM/APP/Sep system.

Figures 17 and 18 shows, respectively, digital photographs and SEM micrographs of the surface of residues for compositions after cone calorimeter test. For all compositions, char structures showing an intumescence character have been formed. From a comparison of the PP/PA/SGM/APP/Sep and PP/PA/SGM/APP/N5 residues, it appears that the char is more porous for the second composition. This porosity may have major consequences on flame retardancy of these samples, since a porous char structure, thus permeable to gases (oxygen and volatile combustible from the sample), could not provide the best performance as barrier effect to protect the underlying material against the flame.

Thus, these pores could accelerate the evolution of gases to feed the spread of flame as well as the pyrolysis of the char and emission of airborne particles. The difference of the total smoke release between these samples is expressed in Fig. 19. The sample with a porous surface (PP/PA/SGM/APP/N5) evolves more quantity of smoke during cone calorimeter test.

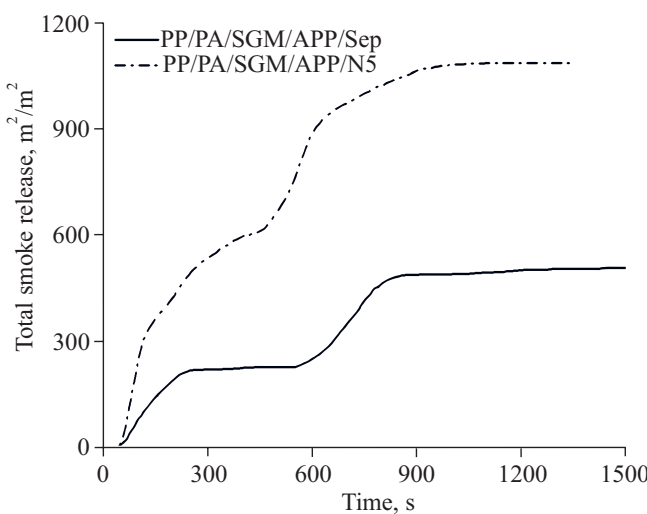


Fig. 19. Total smoke release for PP/PA/SGM/APP/Sep and PP/PA/SGM/APP/N5 samples

The formation of compact charred and expanded structures for the residues seems due to the action of intumescence FR systems which improves the fire reaction of the PP which is the main component of the polymer blend matrix. The main components of these FR systems are the phosphorous compounds acting as acid sources and the PA 6 which acts as a carbon supplier. It has to be noticed that APP appears more effective than OP for almost all compositions. This can be ascribed to the formation of the charred structure at the first stages of PP decomposition, as it can be noticed on TGA and PCFC curves. The thermal stability of the charred structures formed at cone calorimeter which governs the final quantity of residue

could depend on their compact character, according to Huang *et al.* [10]. In addition, it can be considered that the advantage of sepiolite in comparison with other nanoparticles tested could lie in its ability to reinforce mechanically this charred structure at nanometric level and thereby to limit its porosity. It can also be suggested that this enhancement of the quantity of char formed enable more phosphorus to act in the condensed phase, also leading to its reinforcement. Further investigations could concern the evaluation of the mechanical properties of the charred structures formed, the possible formation of new compounds formed by the reaction between the nanoparticles and the phosphorous FRs as well as the phosphorous fraction remaining in the residue.

## CONCLUSIONS

Combinations of nanometric layered silicates such as organomodified montmorillonite and sepiolite with phosphorous FR such as ammonium polyphosphate and aluminum phosphinate allows the fire performances of a compatibilized PP/PA polymer blend to be improved. Conversely, the interest of halloysite, which present a nanotube structure is limited. Although organomodified montmorillonite led to the better performances when the nanoparticles were used without phosphorous FR in the polymer blend, the higher reduction in pHRR, THR, smoke release and the largest residue at cone calorimeter test has been obtained for a sepiolite/ammonium polyphosphate combination. The barrier effect created by the use of sepiolite has been highlighted by a comparison between cone calorimeter and PCFC data. This effect is ascribed to the formation of a very compact charred protective structure, possibly reinforced by the sepiolite fibres, and less porous than this formed with montmorillonite.

## REFERENCES

1. Jiang D.: „Polymer Nanocomposites” Chap. 11 in „Fire Retardancy of Polymeric Materials” (Eds. Morgan A., Wilkie C.), Second Edition, CRC Press 2009.
2. Laoutid F., Bonnau L., Alexandre M., Lopez-Cuesta J.-M., Dubois Ph.: *Mater. Sci. Eng.* 2009, **63**, 100.
3. Kiliaris P., Papaspyrides C. D.: *Prog. Polym. Sci.* 2010, **35**, 902.
4. Laoutid F., Lopez-Cuesta J.-M.: „Multi-components FR systems: polymer nanocomposites combined with additional materials” Chap. 12 in „Fire Retardancy of Polymeric Materials” (Eds. Morgan A., Wilkie C.), Second Edition, CRC Press 2009.
5. Tang Y., Hu Y., Xiao J., Wang J., Song L., Fan W.: *Polym. Adv. Technol.* 2005, **16**, 338.
6. Isitman N. A., Dogan M., Bayramli E., Kaynak C.: *Polym. Degrad. Stab.* 2012, **97**, 1285.
7. Almeras X., Dabrowski F., Le Bras M., Poutch F., Bourbigot S., Marosi G., Anna P.: *Polym. Degrad. Stab.* 2002, **77**, 315.
8. Bourbigot S., Le Bras M., Dabrowski F., Gilman J. W., Kashiwagi T.: *Fire Mater.* 2000, **24**, 201.

9. Tang Y., Hu Y., Li B., Liu L., Wang Z., Chen Z., Fan W.: *J. Polym. Sci. A Polym. Chem.* 2004, **42**, 6161.
10. Tang Y., Hu Y., Song L., Zong R., Gui Z., Fan W.: *Polym. Degrad. Stab.* 2006, **91**, 234.
11. Huang N. H., Chen Z. J., Wang J. Q., Wei P.: *EXPRESS Polym. Lett.* 2010, **4**, 743.
12. Laachachi A., Cochez M., Leroy E., Gaudon P., Ferriol M., Lopez-Cuesta J. M.: *Polym. Adv. Technol.* 2006, **17**, 327.
13. Du M., Guo B., Jia D.: *Polym. Int.* 2010, **59**, 574.
14. Merinska D., Kalendova A., Hromadkova J., Hausnerova B.: „Mechanical and barrier properties of PE and EVA/clay nanocomposites” in „Proceedings of the 5th WSEAS International Conference on Materials Science” (Eds. Marques V. M., Dmitriev A.), Sliema, Malta 2012, pp. 254–259.
15. Gilman J. W.: „Flame retardant mechanism of polymer-clay nanocomposites” in „Flame retardant polymer nanocomposites” (Ed. Morgan A., Wilkie C.), Wiley-Interscience 2007, p. 67.
16. Zanetti M., Lomakin S., Camino G.: *Macromol. Mater. Eng.* 2000, **279**, 1.
17. Laachachi A., Leroy E., Cochez M., Ferriol M., Lopez Cuesta J. M.: *Polym. Degrad. Stab.* 2005, **89**, 344.
18. Lewin M.: *Polym. Adv. Technol.* 2006, **17**, 758.
19. Laachachi A., Cochez M., Leroy E., Ferriol M., Lopez-Cuesta J. M.: *Polym. Degrad. Stab.* 2007, **92**, 61.
20. Schartel B., Pawlowski K. H., Lyon R. E.: *Thermochim. Acta.* 2007, **462**, 1.
21. Morgan A. B., Galaska M.: *Polym. Adv. Technol.* 2008, **19**, 530.
22. Tibiletti L., Longuet C., Ferry L., Coutelen P., Mas A., Robin J. J., Lopez-Cuesta J. M.: *Polym. Degrad. Stab.* 2011, **96**, 67.
23. Sonnier R., Ferry L., Longuet C., Laoutid F., Friederich B., Laachachi A., Lopez-Cuesta J. M.: *Polym. Adv. Technol.* 2011, **22**, 1091.

Received 13 IX 2012.

*Wybrałem rozwiązania Instytutu Tele- i Radiotechnicznego, bo zapewniają:*

**Oferta Instytutu:**

*Technologie materiałów magnetycznych,  
E- systemy dla energetyki, płytki PCB, montaż SMT,  
zgrzewarki ultradźwiękowe, komory próżniowe,  
aparatura cieplno-chemiczna, usługi mechaniczne  
certyfikacja , badania materiałowe.*

**Programowalny Sterownik Polowy Do Sieci Smart Grid- MUPASZ 710 Plus**

**Magnesy produkcji ITR**

**Płytki PCB**

**Instytut Tele- i Radiotechniczny**

03-450 Warszawa  
ul. Ratuszowa 11  
tel: +48 22 619 22 41  
fax: +48 22 619 29 47

**...tworzymy innowacyjne rozwiązania**  
[www.itr.org.pl](http://www.itr.org.pl)